Evaluation of the (UHP)FRC slab contact blast resistance with numerical simulation using LS-DYNA®

Ondřej Janota

Marek Foglar

Faculty of Civili Engineering
Czech Technical University in Prague
Thákurova 7/2007, Prague 16629, Czech Republic

Abstract
Recent development of a security situation in the world and rising numbers of bomb attacks raised new requirements on the material properties and its resistance against blast loads. Commonly used concrete mixtures do not sufficiently meet these requirements. To describe concrete blast resistance and improve it, series of the experiments with full scale specimens were performed. Various concrete specimens made of usually used FRC up to less used UHPFRC were loaded by contact blast. Different concrete mixture attributes as strength, fracture energy or amount of fibres in the specimen and its influence on the blast resistance were evaluated. Results show positive effects of the increased compressive strength and fracture energy on the blast resistance. However, results indicate that blast resitance of the composite slab can be influenced in relatively easier and cheaper manner than by reaching high compressive strength and flexure energy values.

1 Introduction

Experimental measurement of the FRC and UHPFRC slabs loaded by the contact blast took place in 2014, 2015 and 2016 in the Boletice military area. Masurement was performed in the cooperation with the Czech Army and the University of Defence, University of Pardubice.

Experimental measurements were focused on blast resistance of composite panels. Two types of blast load were aplied on each specimen. Firstly, the adjacent blast load experiment was performed in the middle of the specimen. After the evaluation of the adjacent blast experiment, specimen was erected into the vertical position and two contact charges were placed on the side parts of the specimen (Fig. 1).

During the years, eleven specimens, with different material characteristics were tested. Twenty-one contact blasts in total. Each contact experiment was visually evaluated on the site and the damage of the specimen was measured. Visual evaluation was mainly focused on the specimen damage, crack pattern on both sides and reinforcement bars damage. Specimen damage was evalutated on the contact side and soffit as well. Damaged area of the cover layer and the area deeper the the cover layer was measured separately.

1.1 Specimens

Each specimen was made from the reinforced fibre concrete slab with the dimensions 6000 x 1500 x 300 mm. The steel reinforcement was 11 pcs ∅ 16 mm reinforcing bars every 140 mm on both surfaces, ∅ 10 mm every 150 mm as an outer transverse reinforcement, and shear reinforcement was provided by ∅ 8 mm links (9 pcs/m^2). Cover of the stirrups was 50 mm. Amount and type of the dispersed reinforcement, with yield stress 2200 MPa, varies with each specimen as well as the concrete compressive strength. Specimens are named according to their succession in the Boletice blast tests. First tested specimen for the contact blast was specimen No. 12. The last one was No. 23. In the later years of the field experiments, specimens No. 17 – 23 expept No. 21 were suplmeneted with the added elements for the increasement of the heterogeneity. These elements were made from textile sheets or layers of basalt mesh. For short summary of the specimen properties see table 1.

Table 1 Summary of the tested specimens including their properties and weigth of explosive.

Specimen	No.12	No.13	No.14	No.15	No.16	No.17	No.18	No.19	No.21	No.22	No.23
Cubic strength [MPa]	68.5	66.9	73.2	76.1	129.5	125.8	77.9	78.3	127.1	121.6	91.6
Fracture energy [MJ]	13.06	12.36	12.46	13.32	16.35	9.47	6.06	12.20	13.90	8.35	23.16
Fibres length 13 mm kg/m^3]	-	-	-	-	120	80	120	80	80	120	80
Fibres length 35 mm[kg/m^3]	40	80	40	80	-	80	-	80	80	-	-
Fibres length 55 mm[kg/m^3]	-	-	-	-	-	-	-	-	-	-	80
Heterogeneity elements	-	-	-	-	-	Mesh	Mesh-es	Sheets	-	Mesh-es	Sheets
Weight of the explosive [kg] right/left	1.4	0.5	1.4	1.4	2.8	2.8	2.8	2.8	2.8	2.8	2.8
	1.0	1.0	2.8	-	2.0	4.2	4.2	4.2	4.2	4.2	4.2

Fig. 1. Prepared specimen in vertical position with two explosive charges located in the cetre of the both side parts.

2.1 Experimental results

Following paragraphs are presenting dependency of the specimen blast resistance on the particular material properties. Regarding the limited text length of this paper, only selected results are presented. Each material or specimen property influence is presented separately regardless on the other facts. Evaluation of the dependency was performed only for the experiments with 2.8 kilograms and 4.2 kilograms as other weights were tested in a very few tests.

2.1.1 Influence of the compressive strength

According to [1], spalling on the contact side is caused by the punching as the wave propagates into the specimen. On the other hand, on the soffit tensile failure occurs as the wave hits the averted surface and partially bounds back [2] [3]. According to this theory, the cubic strength should influence the damage on the contact side rather than on the soffit. The damage area evolution according to the specimen cubic strength is shown in the Fig. 2.

The results from the experiment verified theory of the different types of failure on both sides. On the contact side, the specimens with the compressive cubic strength higher than 100 MPa have showed to be more resistant than specimens with the lower strength. This trend was seen mostly on the damage area deeper than cover layer. Decrease of the damage area of the specimens with the

strength more than 100 MPa compared to the specimens with the lower strength was approximately 20% on the surface and 50% on the cover layer. This trend was measured mostly for the experiments with the 2.8 kilograms charge. The results from the experiments with the 4.2 kilograms charge showed opposite trend. With the increasing strength of concrete damaged area was also increased This trend was observed on contact side as well as on the soffit.

Influence of the compressive strength on the damage of the soffit (Fig. 3) has shown similar trend as on the contact side only for the experiments with the 2.8 kilograms of the explosive. Experiments with the 4.2 kilograms have shown the opposite trend.

Damage of the specimens on the soffit decreases with the higher strength of the specimen for the 2.8 kilograms experiments. However, the damaged areas not deeper than the cover layer decresed only slightly. The specimens with 2.8 kilograms charge also show decrease of the damage area deeper than the cover layer by approximately 25%. This phenomenon is probably caused by increased tensile strength and the change in the brittleness of the concrete specimens. It is commonly known that UHPC and HPC are more brittle than the normal strength concrete. Increased resistance on the soffit due to the increased tensile strength is degraded by the increased brittleness.

Differences among the specimens with similar compressive strength can be caused by the different amount of the dispersed reinforcement in the specimen or by the added elements e.g. specimen No. 14, No. 18 and No. 19.

There is no clarification for the difference of the result for experiments with the 2.8 and 4.2 kilograms charge, although the statistically inssuficient number of the specimens can play its role.

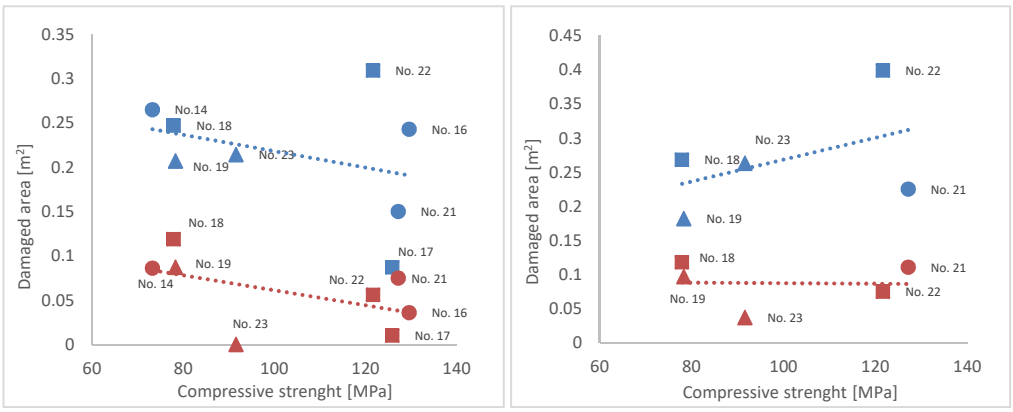

Fig. 2. Dependency of blast resistance on the compressive strength - results on the contact side, Left – 2.8 kilograms tests, Right – 4.2 kilograms tests (blue – damaged area of cover layer, red – damage area deeper than cover layer), (ring – specimens without added elements, triangle – specimens with basalt meshes, square – specimens with textile sheets)

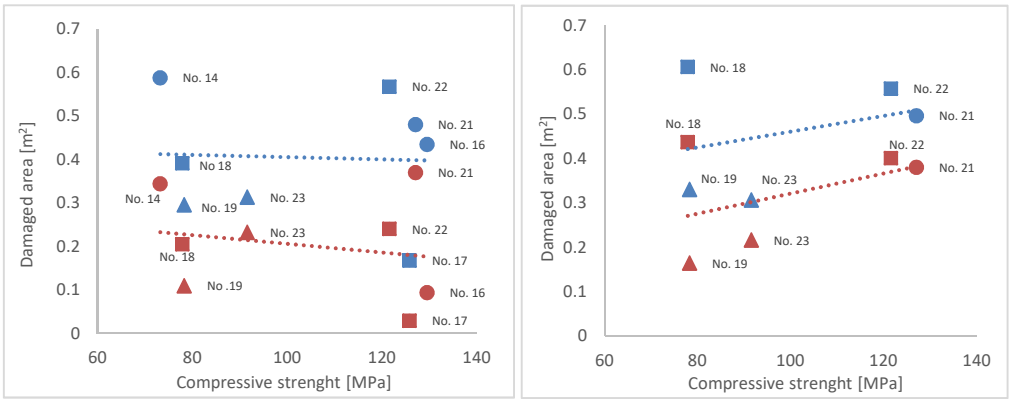

Fig. 3. Dependency of the blast resistance on the compressive strength - results on the soffit, Left – 2.8 kilograms tests, Right – 4.2 kilograms tests (blue – damaged area of cover layer, red – damage area deeper than cover layer), (ring – specimens without added elements, triangle – specimens with basalt meshes, square – specimens with textile sheets)

2.1.2 Influence of the fracture energy

Evaluating influence of the compressive strength separately does not consider the influence of the amount of the dispersed reinforcement and oppositely. Using fracture energy of the FRC should take into account concurrently compressive strength and dispersed reinforcement influence. Evaluation of the fracture energy was performed in the same manner as the compressive strength. According to the theory of the wave propagation through the specimen and types of the failure on the contact side and on the soffit, damage should be influenced by the fracture energy. Fracture energy of the used FRC and UHFRC was derived from the results of the four-point bending tests.

Fig. 4 describes the fracture energy dependency on the final damage of the specimen. It is obvious that the increasing fracture energy decreases damaged zone on the contact side. This progress is especially obvious for the damage deeper than the cover layer where the difference of the damage among the specimens is more than 50%. The specimens No. 16, No. 17 and No. 23 reached the best results especially in the area deeper than the cover layer. The specimen No. 16 and No. 17 was made from UHPFRC with the compressive strength more than 120.0 MPa but its fracture energy was not the highest. The specimen No. 23 was made from UHPFRC with lower compressive strength but with the high amount of fibres, the longest fibres and reached the highest fracture energy.

On the soffit (Fig. 5), the situation is very similar as on the contact side. With the increasing fracture energy, the damage of the specimens decreases. This process was more obvious for the experiments with the weight of charge 4.2 kilograms. Reduction of the damaged area for the specimens with the higher fracture energy in comparison with the specimens with lower fracture energy was around 50%. Results from the experiments with the weight of charge 2.8 kilograms did not agree with the experiments with the charge weight 4.2 kilograms. In the case of the damage area deeper than the cover layer, damage even slightly iincreases with the fracture energy

As well as on the contact side, some specimens made from UHPFRC with lower fracture energy were also less damaged. The best results reached specimens No. 16, No. 17 No. 19 and No. 23. Specimen No. 23 reached the highest value of the fracture energy and its supremancy over other specimens was supposed. However, good result of the specimens No. 16 can be connected to the high compressive strength value, result of the specimens No. 17 and No. 19 could be caused by the added elements. Verification of these phenomenons can lead to better blast resistant material without using materials with very high fracture energy or compresive strength.

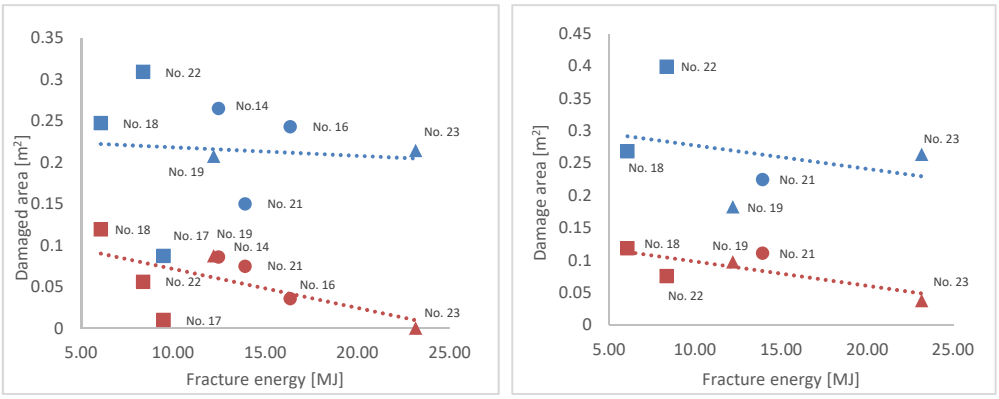

Fig. 4. Dependency of blast resistance on the fracture energy - results on the contact side, Left – 2.8 kilograms tests, Right – 4.2 kilograms tests (blue – damaged area of cover layer, red – damage area deeper than cover layer)

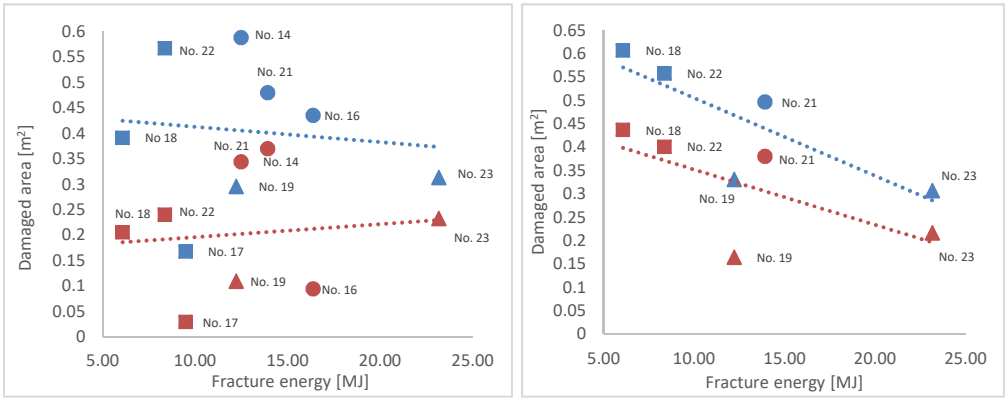

Fig. 5. Dependency of blast resistance on the fracture energy - results on the soffit, Left – 2.8 kilograms tests, Right – 4.2 kilograms tests (blue – damaged area of cover layer, red – damage area deeper than cover layer)

2.1.3 Crack pattern

Cracks were observed mainly on the specimens soffit. According to the visual observations, results can be divided into two groups. The first group (Fig. 6 - left)

is consisted of the specimens with the reinforcement embedded in the concrete after the blast and relatively simple crack pattern on the soffit. There were no cracks or only a few short and quite thin cracks on the specimen surface. Cracks started on the edge of the damaged zone and propagated straight in vertical or horizontal direction. Most of them did not reach the specimens edge. On the surface, cracks were situated in the position of the reinforcement grid.

The second group (Fig. 6 - right) is consisted of the specimens with the reinforcement fully extracted out of concrete. In this case crack pattern was more complex. The surface was heavily cracked around the damaged zone. Most of the cracks started at the point where the rebars started to be embedded in the concrete. Some of them copied the position of the transverse or longitudinal reinforcement but some of them were diagonal to the reinforcement grid. Generally, these cracks can be considered as the radial to the center of the damaged area. Cracks were wider than the cracks in the case

of the first group. Cracks on the specimen upper part and on the side, close to the side edge, often reached tthe specimen edge. On the most of these specimens, part of the radial cracks was connected with one peripheral crack in the variable distance from the parameter of the damaged zone. These peripheral cracks were observed on the specimens with the reinforcement grid strongly bent out of the specimen.

Cause of the cracks in the case of the first group was probably the stress accumulation near the reinforcement as the pressure wave went through. As the rebars stayed embedded in the concrete the cracks were not influenced by the reinforcement bending.

In the second group, radial cracks are supposed to be caused also by the stress accumulation near the rebars and could be widened and prolonged by the reinforcement bending out of the specimen. As the whole reinforcement grid was bent out, the peripheral crack occurred. It is evident that the peripheral cracks occur as the deformation of the rebars go further beyond the damaged area.

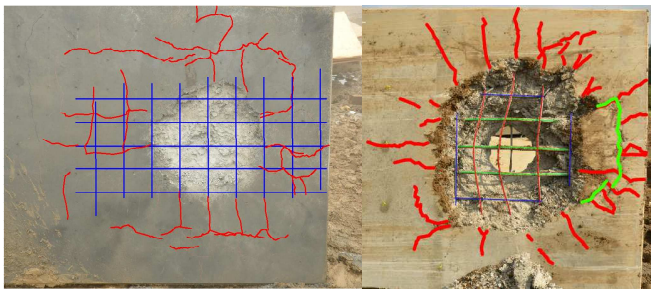

Fig. 6. Left, crack pattern with the cracks copying reinforcement position (blue – reinforcement, red - cracks); Right, crack pattern with radial cracks (bold red) and one peripheral crack (bold green) (blue – little bended reinforcement, thin green and red – heavily bended reinforcement)

3 Numerical simulations

Present-day capabilities in numerical blast simulations offer huge variety of opportunities in the area of the commercial hydrocodes as well as in the area of different blast techniques. For the purpose of the evaluation of the above mentioned phenomenons, the LS-DYNA hydrocode was used. Blast load was simulated with the Smoothed Particle Hydrodynacims method. Specimens No. 14 and No. 21 with the weigth of charge 2.8 kilograms were choosen for the evaluation of the compressive strength and fracture energy influence. Overpressure propagation was also observed.

3.1 Numerical model

The 3D FEM-SPH model was developed for the contact blast simulations. For the conservation of the model size and computational time, the symmetry of the assignment was used. Only part of the specimen with the dimensions 750 x 750 x 300 mm was modeled as well as one quarter of the explosive charge. Neccessity of the symmetry utilization was confirmed as the size of the input file for 5 mm mesh size reached memory limits of the used computer.

Explosive was simulated with the material model *MAT_HIGH_BURN and EOS_JWL. Values for the input were adapted from the [4]. Explosion was simulated with the SPH technique, which is one of the methods suitable for the contact blast simulation.

Specimen was modeled with the 3D solid FEM elements. Mesh size of the elements was set 5 mm in all three dimensions. This size provides adequately accurate results and steel reinforcement can be implemented into the model with no need of mesh adjusting along the specimen. Concrete behaviour was simulted with the *MAT_CONCRETE_DAMAGE_REL3. This material is widely used for the simulation of the dynamic response of concrete and brittle materials. Material behaviour is described with the yield surface, maximum surface and residual surface [5]. Strain-rate, post-peak softening and shear dilatation are also impemented into the material behaviour.

3.2 Results of the numerical simulations

Material model *MAT_CONCRETE_DAMAGE_REL3 does not include inner erosion criterion - element deletion. Thus, fully plasticized elements stay in the model reaching high strains. Implementation of the erosion criterion via *MAT_ADD_EROSION for the better visual simulation of the spalling and punctures has shown as a very complex problem as the implementation influence and devalue the results. Therefore, specimen damage was measured with the effective plastic strain value describing element state among the three stress surfaces.

In the Fig. 7, comparison of the experiment and numerical results is provided. In to upper row damged area (green – cover layer, red – deeper than the cover layer) of the specimens No. 14 and No. 21 and cracks are presented. Both specimens were punctured. There were cracks observed in the case of specimen No. 14 (compressive strenght 78 MPa) but in the case of the specimen No. 21 (compressive strenght 127.1 MPa the cracks did not occur). The comparison of the damge area diamters is presented in table 2.

Bottom row shows the numerical results. Effective plastic strain on the contact side and soffit is displayed. Red area shows fully plasizied elements, blue areas are elements with the effective plastic strain less then 1.5. Diameter of the damaged areas and puncture were considered as the elements with the effective plastic stran 1.9 or higher. Numerical resuls show good agreement with the experimental results. Damage on both surfaces corresponds with the experimentaly measured damage. However, absence of the fragmentation in the numerical model complicates the damage interpretation, especially the puncture.

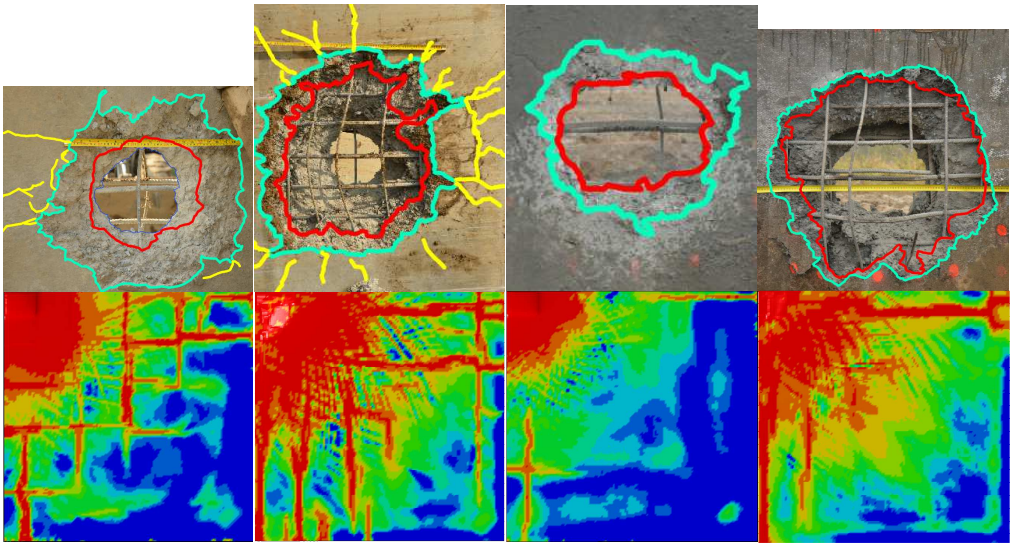

Fig. 7. Comparison of the experimental (top row) and numerical (bottom row) results, Left left - No. 14 contact side, Left right – No. 14 soffit, Right left – No.21 contact side, Right right – No. 21 soffit

Table 2 Comparison of the specimens damage diameters

Specimen	No.14–Exp.	No.14–Num.	Accuarcy	No.21–Exp.	No.21–Num.	Accuarcy
Con. side damage diameter [mm]	489-635	522-612	96.3 -106.7%	350- 463	376-440	95.0-107.4%
Soffit damage diameter [mm]	690-899	658-704	78.3-95.3%	667 - 844	634-892	95.0-105.6%
Puncture diameter [mm]	216-250	230-278	106.5-111.2%	267 - 333	322-342	102.7-120.6%

Crack pattern that can be seen in the Fig. 7 corresponds with the experimental results as well. Both specimens No. 14 surfaces are heavily cracked in contrary to the specimen No. 21 with only a few cracks. Some of the cracks reached the specimen edge. Crack pattern copied the reinforcement

grid in both cases. This could be caused by the absence of the specimen fragmentation. Therefore, reinforcement stays embeden in the concrete, bond with concrete is not lost, and deform equally as the specimen, even if the concrete around is fully plasticized. Cracks near the reinforcement are caused by the wave reflection and different propagation of wave in the steel reinforcement. As the pressure reflects from the reinforcement and propagates easier through the steel, surrounding concrete cracks and cracks propagates further towards the surface. Therefore, the cracks propagation can be considered as opposite to crack propagation caused by the ordinary loading.

4 Conclusion

Results from the full-scale contact blast experiments were presented in this paper. Eleven FRC and UHPFRC slabs with different properties (fracture energy, compressive strength and amount of dispersed reinforcement) were tested. Results are focused mainly on the specimen properties influence on the blast resistance and crack patern on the surface. Numerical simulations of two speciems were used for the evaluation of the observed phenomenons.

Presented results indicate positive influence of the increasing specimen compressive strength as well as flexural energy on contact blast resistance. Compressive strength influences damage on the contact side more than on the soffit. Reduction of the area damage reached around 25% by increasing compressive strength. On the soffit, influence of the compressive strength was less positive. As the scabbing on the soffit is caused by the tensile fracture, which increases with the compressive strength, higher brittleness of the UHPFRC over FRC could play its role.

Fracture energy could also reduce damage of the specimen on both sides thus increasing fracture energy increased the blast resistance. Damage reduction reached around 50%. However, some specimens with lower fracture energy reached better results than the specimens with higher fracture energy. This phenomenon could be caused by the added elements increasing material heterogeneity. Influence of these elements was not described in this paper and needs to be futher investigated.

Two different crack patterns were observed during the experiment. Length, width and direction of the cracks were connected to the classical reinforment.

Numerical simulations performed for the evaluation of the experiment showed good agreement with the experimental model. Two specimens with different compressive strength were compared. Numerical simulations can adequately predict specimen damage and influence of some specimen properties.

Acknowledgements

This work was financially supported by the Grant Agency of the Czech Republic, project no. 17-23067S, which is gratefully acknowledged.

References

[1] XU, Kai a Yong LU. Numerical simulation study of spallation in reinforced concrete plates subjected to blast loading. Computers & Structures [online]. 2006, 84(5-6), 431-438 [cit. 2018-01-14]. DOI: 10.1016/j.compstruc.2005.09.029. ISSN 00457949. Available from: http://linkinghub.elsevier.com/retrieve/pii/S004579490500355X

[2] FOGLAR, Marek a Martin KOVAR. Conclusions from experimental testing of blast resistance of FRC and RC bridge decks. International Journal of Impact Engineering [online]. 2013, 59, 18-28 [cit. 2018-01-15]. DOI: 10.1016/j.ijimpeng.2013.03.008. ISSN 0734743x. Available from: http://linkinghub.elsevier.com/retrieve/pii/S0734743X13000559

[3] FOGLAR, M., J. PACHMAN, V. PELIKAN, R. HÁJEK, M. KÜNZEL a M. KOVAR. The structural response of a reinforced concrete specimen subjected to adjacent blast loading [online]. In: . 2014-06-03, s. 171-179 [cit. 2018-01-15]. DOI: 10.2495/SUSI140151. Available from: http://library.witpress.com/viewpaper.asp?pcode=SUSI14-015-1

[4] DOBRATZ, B. M. a P. C. *LLNL Explosive Handbook: PRoperties of Chemical Explosives and Explosive Stimulants*. Livermore, California: U.S. Department of Commerce, 1985. ISBN 9994811029.

[5] MALVAR, L. J., CRAWFORD J. E., WESEVICH, J. W., SIMONS, D. A New Concrete Material Model for Dyna3D Release II: Shear Dilatation and Directional Rate Enhancements. Glendale, CA: Karagozian & Case, 1996.